Technical University of Denmark

DTU

Large-Eddy Simulation of turbine wake in complex terrain
Paper

Berg, Jacob; Troldborg, Niels; Sørensen, Niels N.; Patton, E. G.; Sullivan, Peter P.

Link back to DTU Orbit

DTU Library
Technical Information Center of Denmark

Large-Eddy Simulation of turbine wake in complex terrain

Large-Eddy Simulation of turbine wake in complex terrain

J. Berg[1], N. Troldborg[1], N.N. Sørensen[1], E. G. Patton[2] and P. P. Sullivan[2]

[1]DTU Wind Energy, Frederiksborgvej 399, 4000 Roskilde, Denmark jbej@dtu.dk
[2] National Center for Atmospheric Research, Boulder, CO, US.

E-mail: `jbej@dtu.dk`

Abstract. We present Large-Eddy Simulation results of a turbine wake in realistic complex terrain with slopes above 0.5. By comparing simulations including and without the wind turbine we can estimate the induction factor, a, and we show how the presence of a strong recirculation zone in the terrain dictates the positioning of the wake. This last finding is in contrast to what would happen in gentle terrain with no substantial increase of turbulent kinetic energy in the terrain induced wakes.

1. Introduction

Wind turbine wakes are characterized by reduced wind speed and increased levels of turbulent kinetic energy. While wind turbine wakes have been studied extensively in homogeneous terrain (and in the absence of terrain) using both Reynolds Averaged Navier-Stokes methods (RANS) [21, 22, 23] and Large-Eddy Simulation methods (LES) [2, 13, 9, 20, 3, 4], only very few modelling studies exist of wakes in complex terrain.

Most of the numerical investigations of rotor wakes in complex terrain are carried out using RANS [12, 5], whereas the only systematic study of accuracy of LES in topography, to our knowledge, has been carried out recently by Shamsoddin and Porté-Agel [15]. In the latter study LES was carried out on five turbines located on a Gaussian hill. Their predictions were compared to measurements obtained in a wind tunnel and rather good agreement was achieved. In the study the hill height to hill half length ratio was 0.5 and the hill height was only about 12% higher than the diameter of the considered turbines. Thus, the complexity of the considered topography in this study is rather limited.

In the present contribution we present LES simulations of the wake of a wind turbine rotor positioned at Perdigão in Portugal - a complex site characterized by a double ridge configuration, and currently the target of a large international measurement campaign under the EU New European Wind Atlas Project[1]. The focus of our work is not the flow around Perdigão as such, but rather the interaction between the terrain and the turbine wake.

2. LES Setup

The LES code is presented in [17, 19]. It is a pseudo-spectral model; wave number representation in the two horizontal directions and finite differencing in the vertical direction. The Boussinesq approximation is adopted and the governing equations are integrated forward in time using

adaptive time stepping (in the current simulations, Δt vary between $0.4\,\mathrm{s}$ and $0.7\,\mathrm{s}$) in a terrain following grid: Whereas the horizontal coordinate lines are Cartesian the vertical z-coordinate is stretched exponentially from the ground and up as a function of the local terrain height. The pressure is solved during an iterative procedure of a general Poisson equation. Compared to running the model on flat terrain ([18]) this last step slows down the code substantially, depending on the complexity of the terrain. We use the Deardorff SGS model in the form as presented by [10] and [16].

2.1. Turbine representaion

In complex terrain we do not have a well defined upstream undisturbed velocity, U_∞, which is often used when estimating the total force the turbine exerts on the flow. Instead we exploit the classical expression [8],

$$U_\infty = \frac{U_d}{1-a},\tag{1}$$

where a is the induction factor and U_d is the velocity on the rotor disk, which can easily be estimated in LES simulations. As in the JHU-LES code [6] turbines are represented by disks with thrust force

$$F_t = -\frac{1}{2}\rho C_T' \langle \bar{u} \rangle_d^2 \frac{\pi}{4} D^2,\tag{2}$$

where C_T' is related through 1-d momentum theory to the thrust coefficient, C_T, and induction factor, a, through

$$C_T' = \frac{C_T}{(1-a)^2} = \frac{4a}{1-a}.\tag{3}$$

D is the rotor diameter and $\langle \bar{u} \rangle_d$ is the rotor area averaged streamwise wind speed. Since a wind turbine act as a low pass filter we also averaged in time: a 10-minute exponential time filter is applied, and its effect on $\langle \bar{u} \rangle_d$ from a LES simulation can be observed in Figure 1. Its effect on the wake loss, however, is almost negligible (not shown in this paper).
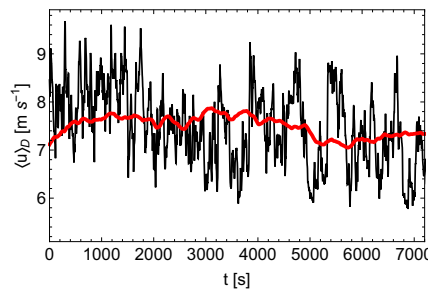
Figure 1: Rotor disk velocity, $\langle u \rangle_d$ with (*red*) and without time averaging (*black*)

In this paper we choose $a = 1/4$ corresponding to $C_T = 3/4$ and finally $C_T' = 4/3$.

The force is distributed proportional to the fractional cross area, ξ, of a given cell covered by the rotor. The force per unit volume in the x direction (perpendicular to the rotor plane) applied to a given cell with indices, (i, j, k), then becomes

$$f_x(i,j,k) = -\frac{1}{2}\rho C_T' \langle \bar{u} \rangle_d^2 \frac{\xi(j,k)}{\Delta x},\tag{4}$$

where Δx is the length of the cell.

2.2. Cases and model spin-up

The simulations are carried out on a $256 \times 128 \times 128$ grid spanning $5120 \times 2560 \times 3000 \, \text{km}^3$ on a terrain representing the double ridge Perdigão in Portugal ([24]). The terrain is smoothed (maximum slope is 0.57) with an exponential filter in wave number space in order to reduce the number of pressure iterations in the code, and hence reduce computer time. Since the focus of this contribution is on turbine wake interaction and not on the precise details of the flow around Perdigão, we do not consider this an issue.

The driving pressure gradient is held constant throughout the study at $dP/dx = -u_\star^2/H$, where $u_\star = 0.6 \, \text{m s}^{-1}$ and $H = 3000 \, \text{m}$ is the height of the computational domain. With $z_0 = 0.5 \, \text{m}$ we have $z_0/H = 1.67 \times 10^{-4}$. The simulations were started from an initial random incompressible velocity fields and ran for approximately $T_S = 100 \, T_E$, with $T_E = H/u_\star$ before time stationarity was obtained. The periodic boundary conditions are maintained by adding a small buffer zone to the terrain. In this way we can ensure that there are no large gradients in the terrain height between the last row and the first row and between the last column and the first column of the terrain file. We have also tried to increase the buffer zone considerably, but did not observe any significant changes to the results presented in this paper (not shown). Since Perdigão is a highly complex site (there is always another bump on the road upstream) running with periodic boundary conditions might even be a more realistic option compared to a well defined inlet condition as is often the case in complex terrain studies [7]. Alternatively, precursor simulations similar to what was introduced by Munters et al. in [11] could be used, although the non-homogeneity of the terrain would add another layer of complexity.

In Figure 2 we show the terrain around Perdigão and in Figure 3 a snapshot of the instantaneous streamwise velocity component along the main transect. The wind direction is from the south west at 235 degrees along the main transect.
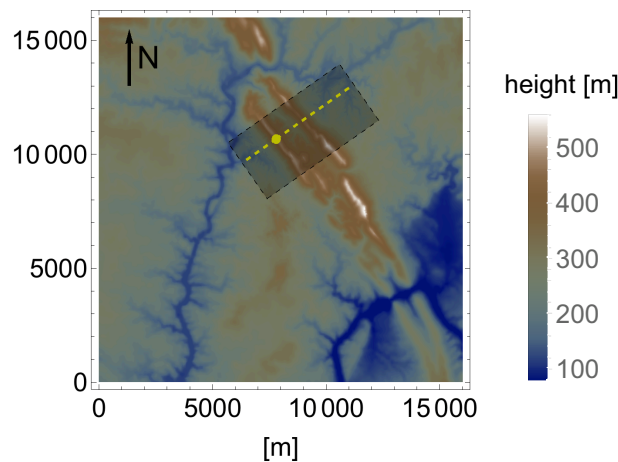
Figure 2: Perdigão terrain heights. The simulated area is represented by the shaded rectangle and the yellow line is the main transect.

3. Data

We analyse averaged LES data. The wind turbine is located on the first ridge as in reality. The average streamwise velocity and resolved turbulent kinetic energy from simulation without the presence of the wind turbine are plotted in Figure 4. The average is taken 10 hours of simulated real-time. With slopes above 0.5 the terrain is challenging and flow separation is
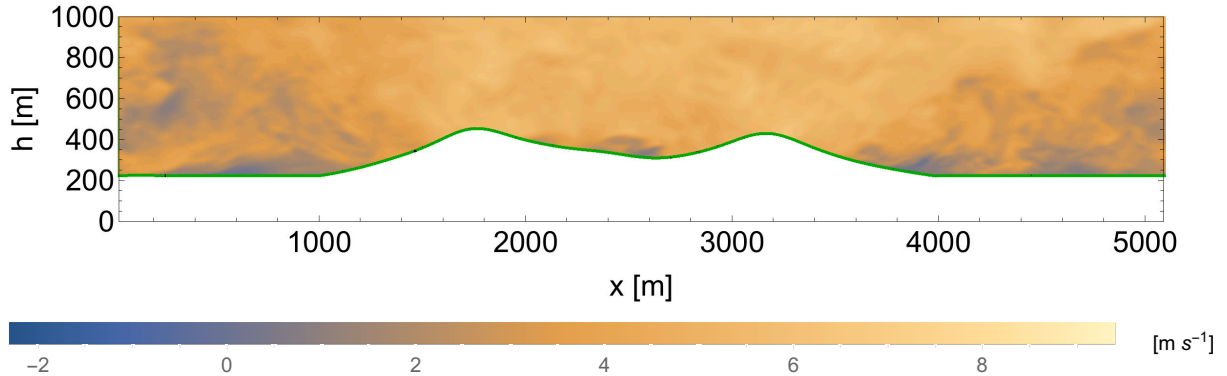
Figure 3: Instantaneous streamwise velocity along the main transect presented in Figure 2 from LES simulation without wind turbine.

present behind the ridge with associated recirculation zone and enhanced turbulence. The exact size and position of the recirculation zone is strongly dependent of the specific smoothing technique performed to the terrain as well as on the spatial resolution (not shown).

Figure 4: Average streamwise velocity without turbine along main transect (*left*) and resolved turbulent kinetic energy (*right*). The turbine position (not present in the simulation here) and downstream distances $1D$, $2.5D$ and $5D$ are shown for illustration.
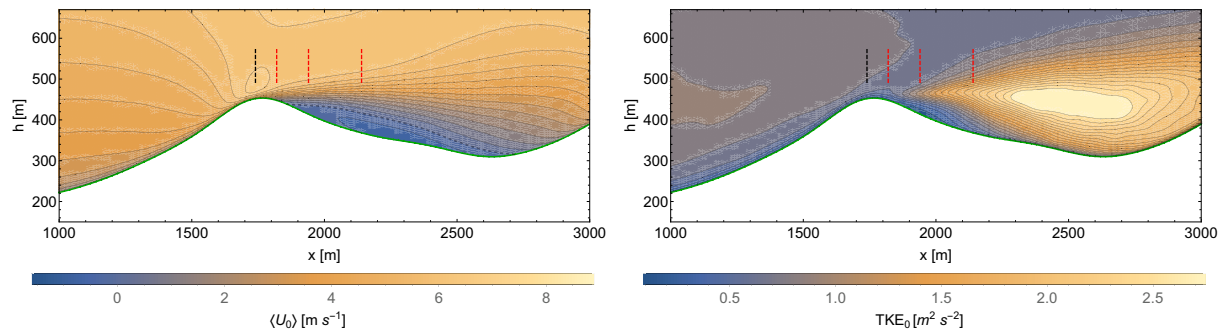
In Figure 5 we compare the flow field around the first ridge with and without a wind turbine. The trouble in estimating the undisturbed velocity, U_∞ in eq. 1 motivates the definition of an alternative induction factor, $\tilde{a}$, defined as

$$\tilde{a} = \frac{\langle U_0 \rangle - \langle U_1 \rangle}{\langle U_{0,hub} \rangle}, \tag{5}$$

where $\langle U_0 \rangle$ and $\langle U_1 \rangle$ are the velocities from the LES simulations without and including the wind turbine, respectively. The denominator velocity is evaluated at hub height equal to $80\,\mathrm{m}$. Since LES simulations are random in nature (here understood in the sense that individual realizations - here 30-min simulations - are different [25]), the quantities in eq. 5 are time dependent, and we have therefore used the velocity in the simulation without the wind turbine in the same time 30-min interval as the one including the wind turbine at the position of the wind turbine, i.e. on top of the first ridge.

In the left panel we observe induction factors on the disk slightly above the target value of 0.25, which is dictated by classical one dimensional momentum theory. The resolved turbulent

kinetic energy presented in the right panel indicate expected enhanced production in the shear layers of the turbine wake, especially above the turbine, where a very strong narrow band is observed. The far wake is slightly pointing upwards. This fits the observations in Figure 4 where the narrowing of streamlines behind the hill above the flow separation zone enhances the turbulent kinetic energy extending to higher elevations compared to the hill height.

In Figure 6 we present plots of $\tilde{a}$ at fixed positions downstream. The error bars indicate the standard deviation of the many 30-min runs analysed. We observe quite large deviations in $\tilde{a}$ within the different 30-min runs.

In Figure 7 we observe how the wake stays more or less at fixed positions in the $y - z$ plane with only a slight move to the right for distances above $2.5D$. It thus follows the geometry of the terrain, which is almost symmetric around the main transect.

In Figure 13 and 15 of [15] it is observed how the wakes more or less follow the terrain, which in all cases are more gentle than the terrain in our study. Here, we show in contrary that the complexity of the terrain and the strong recirculation zone behind the ridge creates a strong shear layer which prevents the wake from following the terrain and blend with the wake of the ridge (besides a small region of excess turbulent kinetic energy present around $x \sim 2000\,\mathrm{m}$).
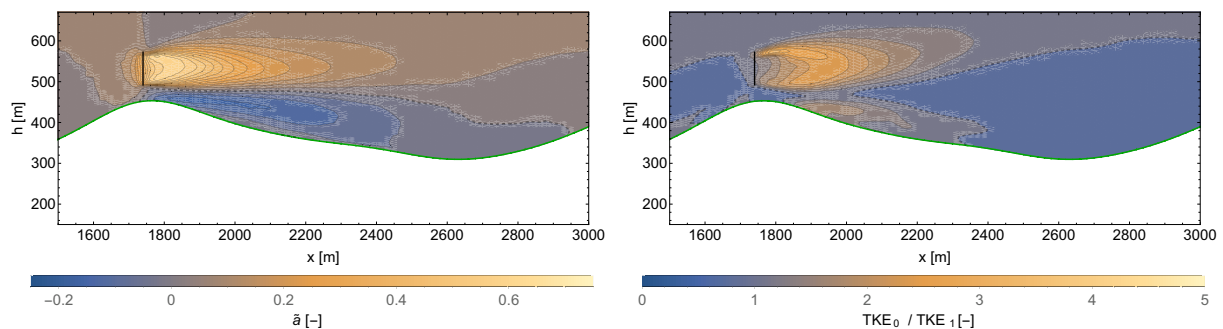

Figure 5: 30-minutes average plots of $\tilde{a}$ (*left*) and ratio of turbulent kinetic energy, TKE between simulations with and without the wind turbine (*right*). The dashed lines indicate where $\tilde{a} = 0$ (*left*) and where the TKE ratio equals one (*right*).

4. Outlook

In the near future there will be measurements of the turbine wake itself at Perdigão. This will provide us with data that can be used to validate the results presented in this contribution. Another aspect that needs attention is whether the turbine representation used in this paper is too simplified: in complex terrain the mean wind is rarely horizontal and do not always follow the largest gradients in the terrain. In addition the inclusion of Coriolis force, stratification and inversion strength will force us to use a PID controller somewhat similar to what is presented in [14]. Perdigão also poses a challenge when it comes to resolution and domain size. The complexity and size of the terrain features of interest makes it computational very expensive if smaller scales are to be resolved while keeping the size of the domain constant. It is expected that the flow around Perdigão will change when we obtain a higher resolution and less smoothing (work in progress). The interaction with the wake will also change as a consequence. Thus in order to really numerically study the interaction between turbine wakes and realistic complex terrain as present at Perdigão much computer power is needed.
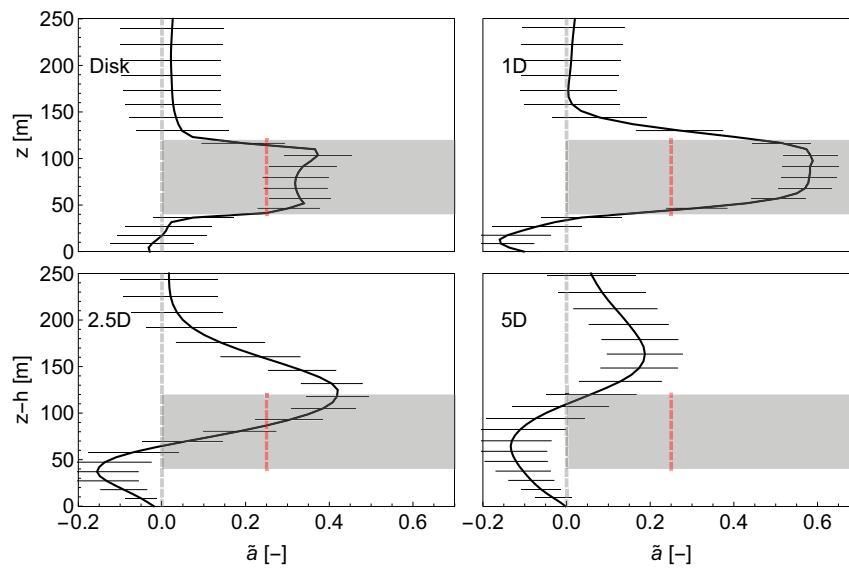
Figure 6: Profiles of the induction factor, $\tilde{a}$, at fixed positions downstream from the turbine. The rotor area is indicated by the gray shading and the red line indicates the $a = 0.25$. Error bars indicate the standard deviation.

Figure 7: $\langle U_1 \rangle$ at fixed distances downstream of the rotor. The black circle represent the position and size of the rotor

References

[1] http://www.neweuropeanwindatlas.eu.

[2] M. Abkar, A. Sharifi, and F. Porté-Agel. Wake flow in a wind farm during a diurnal cycle. *J. Turbulence*, 17:420–441, 2016.

[3] D. Allaerts and J. Meyers. Large eddy simulation of a large wind-turbine array in a conventionally neutral atmospheric boundary layer. *Physics of Fluids*, 27:065108, 2015.
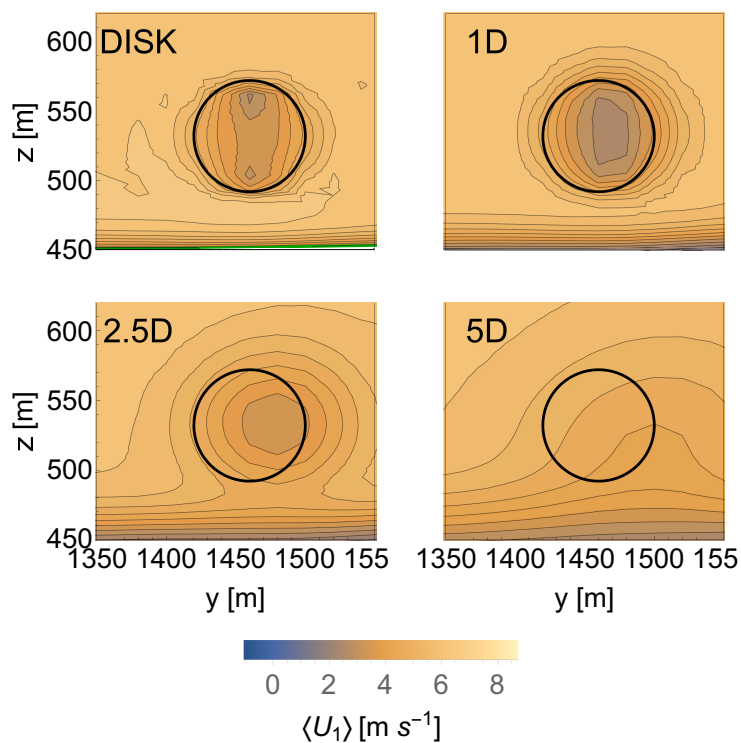
[4] D. Allaerts and J. Meyers. Boundary-layer development and gravity waves in conventionally neutral wind farms. *J. Fluid Mech.*, 814:95130, 2017.

[5] D. Cábezon, K.S. Hansen, and R.J. Barthelmie. Analysis and validation of CFD wind farm models in complex terrain . Effects induced by topography and wind turbines. *EWEC 2010*, pages 1–4, 2008.

[6] M. Calaf, C. Meneveau, and J. Meyers. Large eddy simulation study of fully developed wind-turbine array boundary layers. *Physics of Fluids*, 22(1):1–16, 2010.

[7] D. Cavar, P.-E. Réthoré, A. Bechmann, N. N. Sørensen, B. Martinez, F. Zahle, J. Berg, and M. C. Kelly. Comparison of openfoam and ellipsys3d for neutral atmospheric flow over complex terrain. *Wind Energy Science*, 1(1):55–70, 2016.

[8] M. O. L. Hansen. *Aerodynamics of Wind Turbines, 3.ed.* Routledge, Taylor Francis Group, 2015.

[9] S. Lee, M. Churchfield, P. Moriarty, J. Jonkman, and J. Michalakes. A Numerical Study of the Effects of Atmospheric and Wake Turbulence on Wind Turbine Dynamics. *J. Turbulence*, 13:1–32, 1989.

[10] C.-H. Moeng. A large-eddy-simulation model for the study of planetary boundary-layer turbulence. *Journal of the Atmospheric Sciences*, 41(13):2052–2062, 1984.

[11] W. Munters, C. Meneveau, and J. Meyers. Turbulent inflow precursor method with time-varying direction for large-eddy simulations and applications to wind farms. *Boundary-Layer Meteorology*, 159(2):305–328, 2016.

[12] E.S. Politis, J. Prospathopoulos, D. Cabezon, Kurt Schaldemose Hansen, P.K. Chaviaropoulos, and R.J. Barthelmie. Modeling wake effects in large wind farms in complex terrain: the problem, the methods and the issues. *Wind Energy*, 15(1):161–182, 2012.

[13] F. Porté-Agel, Y-T. Wu, H. Lu, and R.J. Conzemius. Large-eddy simulation of atmospheric boundary layer flow through wind turbines and wind farms. *J. Wind Eng. Ind. Aerodyn*, 99:154–168, 2011.

[14] A. Sescu and C. Meneveau. A control algorithm for statistically stationary large-eddy simulations of thermally stratified boundary layers. *Q. J. R. Meteorol. Soc.*, 140(683):2017–2022, 2014.

[15] S. Shamsoddin and F. Porté-Agel. Large-eddy simulation of atmospheric boundary-layer flow through a wind farm sited on topography. *Boundary-Layer Meteorol.*, 163(1):1–17, 2017.

[16] P. P. Sullivan, J. C. McWilliams, and Chin-Hoh Moeng. A subgrid-scale model for large-eddy simulation of planetary boundary-layer flows. *Boundary-Layer Meteorol.*, 71:247–276, 1994.

[17] P. P. Sullivan, J. C. McWilliams, and E. G. Patton. Large eddy simulation of marine atmospheric boundary layers above a spectrum of moving waves. *J. Atmos. Sci.*, 71:4001–4027, 2014.

[18] P. P. Sullivan and E. G. Patton. The effect of mesh resolution on convective boundary layer statistics and structures generated by large-eddy simulation. *J. Atmos. Sci.*, 68:2395–2415, 2011.

[19] P.P. Sullivan, E.G. Patton, and K.W. Ayotte. Turbulent flow over and around sinusoidal bumps, hills, gaps and craters derived from large eddy simulations. In *19th Conference on Boundary Layer and Turbulence, Keystone, CO*, 2010.

[20] N. Troldborg, F. Zahle, P-E Réthoré, and N.N Sørensen. Comparison of wind turbine wake properties in non-sheared inflow predicted by different computational fluid dynamics rotor models. *Wind Energy*, 2014.

[21] M. P. van der Laan, N. N. Sørensen, P.-E. Réthoré, J. Mann, M. C. Kelly, and N. Troldborg. The k-ε-f_p model applied to double wind turbine wakes using different actuator disk force methods. *Wind Energy*, 18(12):2223, December 2015.

[22] M. P. van der Laan, N. N. Sørensen, P.-E. Réthoré, J. Mann, M. C. Kelly, N. Troldborg, K. S. Hansen, and J. P. Murcia. The k-ε-f_p model applied to wind farms. *Wind Energy*, 18(12):2065, December 2015.

[23] M. P. van der Laan, N. N. Sørensen, P.-E. Réthoré, J. Mann, M. C. Kelly, N. Troldborg, J. G. Schepers, and E. Machefaux. An improved k-ε model applied to a wind turbine wake in atmospheric turbulence. *Wind Energy*, 18(5):889, May 2015.

[24] N. Vasiljević, J. M. L. M. Palma, N. Angelou, J. C. Matos, R. Menke, G. Lea, J. Mann, M. Courtney, L. F. Ribeiro, and V. M. M. G. C. Gomes. Perdigão 2015: methodology for atmospheric multi-doppler lidar experiments. *Atmos. Meas. Tech. Discussions*, 2017:1–28, 2017.

[25] John C. Wyngaard. *Turbulence in the Atmosphere.* Cambridge University Press, 2010.